



Article

Optimisation of PLS Calibrations for Filtered and Untreated Samples towards In-Line Monitoring of Phenolic Extraction during Red-Wine Fermentations

Kiera Lambrecht¹, H el ene Nieuwoudt¹, Wessel du Toit¹ and Jos e Luis Aleixandre-Tudo^{1,2,*}

¹ South African Grape and Wine Research Institute (SAGWRI), Department Viticulture and Oenology, University of Stellenbosch, Private Bag X1, Matieland, Stellenbosch 7602, South Africa; kieranareece@sun.ac.za (K.L.); hhn@sun.ac.za (H.N.); wdutoit@sun.ac.za (W.d.T.)

² Instituto de Ingenier a de Alimentos para el Desarrollo (IIAD), Departamento de Tecnolog a de Alimentos, Universitat Polit cnica de Valencia, Camino de Vera s/n, 46022 Valencia, Spain

* Correspondence: joaltu@sun.ac.za

Abstract: Infrared spectroscopy provides an efficient, robust, and multivariate means to measure phenolic levels during red-wine fermentations. However, its use is currently limited to off-line sampling. In this study, partial least squares (PLS) regression was used to investigate the possibility of using spectral data from minimally pre-treated or untreated samples for the optimisation of prediction calibrations towards an in-line monitoring set-up. The evaluation of the model performance was conducted using a variety of metrics. Limits of detection and quantification of the PLS calibrations were used to assess the ability of the models to predict lower levels of phenolics from the start of fermentation. The calibrations were shown to be useful for the quantification of phenolic compounds and phenolic parameters with minimal or no sample pre-treatment during red-wine fermentation. Upon evaluation of performance, the calibrations built for attenuated-transmission Fourier-transform mid-infrared (ATR-FT-MIR) and diffuse-reflectance Fourier-transform near-infrared (DR-FT-NIR) were shown to be the most suitable spectroscopy techniques for eventual application in an automated and in-line system with values for limits of detection and quantification being suitable for the entire duration of fermentation.

Keywords: spectral pre-processing; PLS regression; infrared spectroscopy; phenolic compounds; limit of detection



Citation: Lambrecht, K.; Nieuwoudt, H.; du Toit, W.; Aleixandre-Tudo, J.L. Optimisation of PLS Calibrations for Filtered and Untreated Samples towards In-Line Monitoring of Phenolic Extraction during Red-Wine Fermentations. *Fermentation* **2022**, *8*, 231. <https://doi.org/10.3390/fermentation8050231>

Academic Editor:  ngela Fernandes

Received: 29 March 2022

Accepted: 27 April 2022

Published: 17 May 2022

Publisher's Note: MDPI stays neutral with regard to jurisdictional claims in published maps and institutional affiliations.



Copyright:   2022 by the authors. Licensee MDPI, Basel, Switzerland. This article is an open access article distributed under the terms and conditions of the Creative Commons Attribution (CC BY) license (<https://creativecommons.org/licenses/by/4.0/>).

1. Introduction

Winemaking has been a part of civilisation since as early as 6000 BC, with signs of winemaking practices being documented in Mesopotamia and Caucasus [1]. In modern times, winemaking is a worldwide industry, with many countries being frontrunners [2]. As such, this leads to a highly competitive global market, where consistency and quality are required by the wine buyers [3].

With new technologies becoming available and rapid improvement in software and computing, more methods to monitor parameters of oenological importance have become available and more widely used. In particular, the use of spectroscopic technologies is becoming commonplace, with infrared and fluorescence being applied to many industries [4]. Due to their availability, robustness, and non-destructive nature, near-infrared (NIR) and mid-infrared (MIR) spectroscopy in conjunction with chemometrics has become an area of interest in both industrial and research communities for this purpose [5–10]. As with most industrial processes, the control of the winemaking process is essential to avoiding problems that may arise leading to low-quality wines and, therefore, the loss of a competitive edge [11]. Previously, time-consuming and, often, destructive methods were used to quantify certain phenolic and oenological parameters during fermentation [7].

Phenolic components present in wine contribute to the sensory qualities such as mouthfeel, colour, and taste [12,13]. As such, measuring and monitoring the extraction of these compounds during fermentation is an important aspect to ensuring that quality parameters are achieved and process control is maintained [9,14]. Robust and multivariate models utilising both NIR and MIR instrumentation have been developed to quantify oenological parameters; however, these rely on discrete samples that have received treatments to remove particles in suspension [11,15,16]. To our knowledge, there have been no attempts to build or optimise PLS calibrations for phenolic parameters or the concentration of phenolic compounds in minimally treated (filtered) or untreated red-wine samples using infrared spectroscopy.

In a previous study, the effect of different sample treatments on spectral data was evaluated [17]. Promising PLS calibrations were built for the quantification of phenolic parameters during wine fermentation using samples that received different sample treatments, in the form of freezing, centrifugation and filtration. The purpose of this study is to further move towards automated and in-line methods of analysis by optimising calibrations with spectral data from samples receiving minimal (rough filtration) or no treatment, as these would more accurately represent measurements taken directly from a fermentation vessel. The robustness and accuracy of the models and whether the models are applicable during the entire duration of the fermentation, especially from the very beginning when lower phenolic levels are present, was evaluated. The limit of detection and quantification was therefore assessed and considered during the optimisation process. The suitability of three different infrared spectroscopic techniques for in-line implementation, namely attenuated-transmission Fourier-transform mid-infrared (ATR-FT-MIR), transmission Fourier-transform near-infrared (T-FT-NIR) and diffuse-reflectance Fourier-transform near-infrared (DR-FT-NIR), was investigated. ATR-FT-MIR was selected as one method as it has shown promise regarding turbid and opaque samples and would be suitable for an in-line application. For the NIR technologies, the diffuse-reflectance method was chosen due to its contactless nature, allowing for the non-invasive analysis of samples. Finally, the T-FT-NIR technology was chosen as the availability of the liquid probe attachment could potentially lend itself to installation in piping and tanks in industrial applications [17].

2. Materials and Methods

2.1. Small-Scale Vinifications and Sample Treatment

One hundred and twenty kilograms of Shiraz and Cabernet Franc grapes were collected from a collaborating cellar in the Stellenbosch region of South Africa. Before crushing and destemming took place, the grapes were stored at 4 °C for two days. To ensure homogeneity between the 20 kg fermentations, the juice and skins of each cultivar were mixed thoroughly in a bin after crushing and destemming before subdivision. Once subdivided, the SO₂ concentration was adjusted to 30 ppm using a 2% SO₂ solution. Each fermentation was moved into a fermentation room held at 25 °C. A strain of *Saccharomyces cerevisiae* Lalvin ICV D21[®] (Lallemand, Montreal, QC, Canada) was used for alcoholic fermentation. Inoculation was performed according to manufacturer's instructions. This yeast was chosen due to its suitability for producing red wines with stable colour, as well as its high alcohol tolerance and good fermentative performance.

Half of the fermentations received enzymatic treatments at the same time as inoculation with *S. cerevisiae*. The enzyme used was Lafase[®] HE Grand CRU Vin Rouge (Laffort, Bordeaux, France), consisting of pectolytic enzymes, and rehydration and dosing was performed according to manufacturer's instructions. During the AF, three punch downs were done at 08:00, 12:00 and 16:00 each day until alcoholic fermentation was completed. Samples were collected immediately after the 08:00 punch down and during 9 days of fermentation. Briefly, the sample was subdivided into equal volumes and each volume received different pre-treatments. The two pre-treatments of interest for this study were filtration through a 400 µm mesh (Xylem Floject Process Pump Filter, RS Components) and

no pre-treatment (direct sample from the fermenting vessel). Two-millilitre samples were used for ATR-MIR spectroscopy whilst 20 mL samples were used for FT-NIR spectroscopy.

2.2. Spectral Data Acquisition

2.2.1. ATR-FT-MIR Spectroscopy

An Alpha-P Attenuated Total Reflectance Fourier Transform Mid Infrared (ATR-FT-MIR) spectrometer (Bruker Optics, Ettlingen, Germany) with a 2 mm² single bounce diamond sample plate was used to obtain the spectra in a closed environment. A resolution of 4 cm⁻¹ was used over a range of 4000–400 cm⁻¹ and 128 sample scans at a temperature of 30 °C were acquired. The resolution was chosen as it provided well-defined spectra whilst also allowing for time-efficient scanning. Prior to sample scanning, a background spectrum was obtained using distilled water and was repeated every 2 h. All control and selections were performed using OPUS Wine Wizard (OPUS v7.0 for Microsoft, Bruker Optics, Ettlingen, Germany). The average ATR-FT-MIR spectra for filtered and untreated samples are reported in Figure 1.

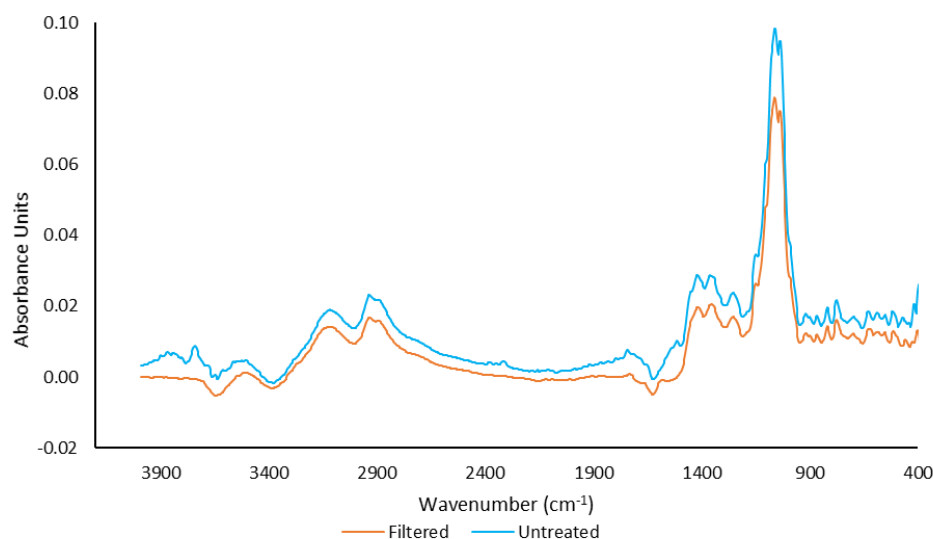


Figure 1. Average filtered and untreated spectra for ATR-FT-MIR spectroscopy.

2.2.2. Transmission FT-NIR Spectroscopy

Transmission Fourier-transform near-infrared (T-FT-NIR) was performed using the liquid probe attachment of the Multi-purpose analyser (MPA) FT-NIR instrument (Bruker Optics, Ettlingen, Germany). A resolution of 2 cm⁻¹ was used over a range of 12,500–4000 cm⁻¹ for 64 sample scans at ambient temperature. An air background spectrum was taken prior to scanning and then every two hours. All control and selections were made using OPUS for Microsoft, Bruker Optics, Ettlingen, Germany). The average T-FT-NIR spectra for filtered and untreated samples are reported in Figure 2.

2.2.3. Diffuse-Reflectance FT-NIR Spectroscopy

Spectra were also collected using a contactless Matrix DR-FT-NIR spectrometer in diffuse-reflectance mode (DR-FT-NIR) (Bruker Optics, Ettlingen, Germany). For sample scanning, two of the four existing tungsten bulbs (12 V, 20 W) were used with a 17 cm measuring distance. A background spectrum was obtained prior to scanning using a 20 mL volume of distilled water in a clear glass container. Sixty-four sample scans were performed over a wavenumber range of 12,500–4000 cm⁻¹ at a resolution of 16 cm⁻¹. The average DR-FT-NIR spectra for filtered and untreated samples are reported in Figure 3.

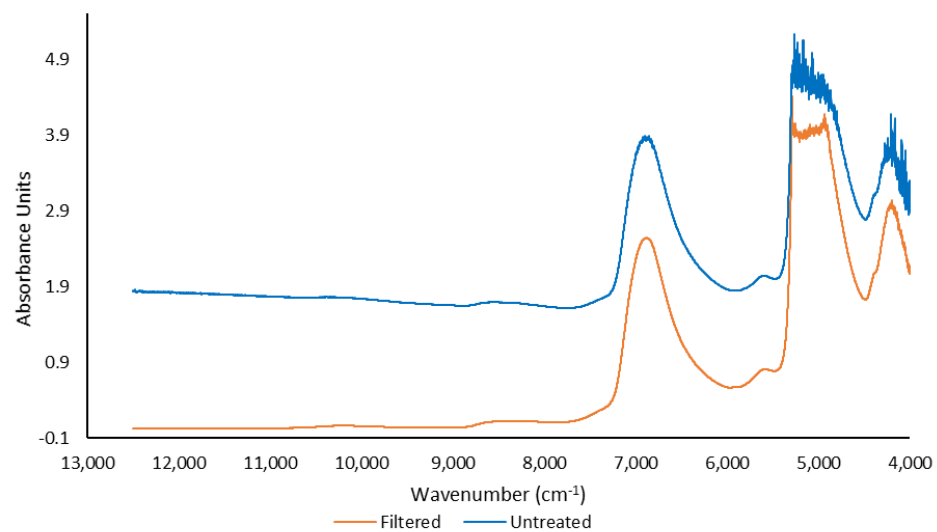


Figure 2. Average filtered and untreated spectra for T-FT-NIR spectroscopy.

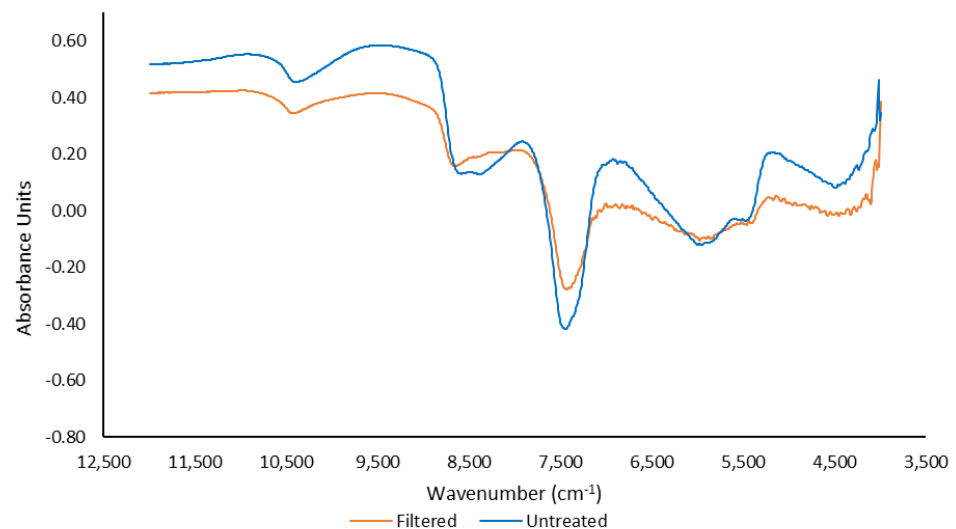


Figure 3. Average filtered and untreated spectra for DR-FT-NIR spectroscopy.

2.3. Iland Analysis for Total Anthocyanin and Total Phenolic Content

For the quantification of total anthocyanin content as well as the total phenolic index of the samples, the method reported by Iland et al. (2000) was used [15,18]. Briefly, this involves the dilution of a 100 μL sample of fermenting must in 5 mL of 1 M HCl after centrifugation of the sample. This is then left in the dark for one hour [19]. A Multiskan GO Microplate Spectrophotometer (Thermo Fisher Scientific, Inc., Waltham, MA, USA) was used to measure the absorbances of 200 μL of the samples at 520 nm and 280 nm for each component, respectively. To obtain the total phenolics index (TPI), the absorbance measured at 280 nm was multiplied by the dilution factor. The anthocyanin content was quantified in terms of malvidin-3-glucoside equivalents, with the use of the following equation [15]:

$$\text{Anthocyanins (mg/L)} = (\text{A}_{520 \text{ nm}} \text{ MW DF}) / (\epsilon \times L) \quad (1)$$

where $\text{A}_{520 \text{ nm}}$ refers to the measured absorbance at 520 nm, MW and ϵ refer to the molecular weight of malvidin-3-glucoside (529 g/mol) and the extinction coefficient (28,000 L/(cm mol)) of this compound, respectively, DF represents the dilution factor and L refers to the 1 cm pathlength used.

2.4. Methylcellulose-Tannin-Precipitation Assay

The concentration of tannins in the samples was quantified using a high-throughput method adapted by Mercurio, Dambergs, Herderich, and Smith (2007). The reagents required for this include a 0.04% *w/v* methylcellulose solution as well as a saturated ammonium-sulphate solution [20]. The method requires both a control receiving no methylcellulose and a treated sample receiving the solution. To prepare the control, a 50 μL measure of a sample was added to a 2 mL microfuge tube, followed by 400 μL of the saturated ammonium-sulphate solution and, finally, topped up with 1550 μL of distilled water. Preparation of the sample receiving treatment involved adding 600 μL of the methylcellulose solution to a 50 μL measure of the sample. After an elapsed time of three minutes, 400 μL of saturated ammonium sulphate was added and 950 μL of distilled water was used to bring the volume to 2 mL. Both control and treatment were centrifuged at $11,180 \times g$ for 5 min using an Eppendorf 5415 D (Hamburg, Germany) centrifuge after allowing precipitation of the tannins to occur (10 min). The absorbances at 280 nm was measured for both the control and treatment. The difference between these values was used to determine the concentration of tannins with the use of a calibration curve using epicatechin equivalents and multiplication by the dilution factor. This calibration curve was generated by making a 1 g/L epicatechin (E1753, Merck, Darmstadt, Germany) stock solution using 0.1 g of epicatechin and 100 mL of 96.4% ethanol. This stock solution was further used to make a dilution series with concentrations in the range 0.025 g/L–0.3 g/L. Two-hundred microliters of each solution in the dilution series was scanned at 280 nm using distilled water as a blank.

2.5. Colour Density

Fifty μL of each sample was pipetted into a 96-well microplate (Thermo Fisher Scientific, Inc., Waltham, MA, USA) and the total absorbance measured at 420 nm, 520 nm and 620 nm with distilled water as a blank. The sum of these absorbances yielded the colour density [21].

2.6. SO_2 -Resistant Pigments

To quantify the concentration of SO_2 -resistant pigments in a sample, the modified Somers Assay, adapted by Mercurio, Dambergs, Herderich, and Smith (2007), was used. A buffer solution consisting of model wine (0.5% *w/v* tartaric acid and 12% *v/v* ethanol adjusted to a pH of 3.4 using 1 M NaOH solution) was used. A 200 μL measure of a sample was diluted with 1.8 mL of the buffer solution with 0.375% *w/v* sodium metabisulphite [20]. After addition of reagents and vortexing, the samples stood for an hour at room temperature. Finally, the absorbance of 200 μL at 520 nm was measured. Using the previous equation for anthocyanin quantification, the final levels of SO_2 -resistant pigments were obtained.

2.7. Development and Validation of PLS Calibrations

All modelling and evaluation of the models were performed using PLS Toolbox 8.8 for MATLAB R2019b (Mathworks Inc., Natick, MA, USA). The data set was split into a calibration and test set with a ratio of 66/34, respectively. For the calibration, the optimal number of latent variables was calculated using a cross-validation procedure. For this, the venetian-blinds approach was used with 10 data splits. To determine the best pre-processing method and wavenumber selection for a particular variable, pre-processing algorithms (including no pre-processing) were considered using both forward and backward iPLS interval selection. The pre-processing options and interval selection that corresponded with the lowest root mean square error (RMSECV) were selected for further model optimisation.

Certain statistics were used to determine the accuracy and reliability of the models. The coefficient of correlation for calibration (R^2_{cal}) and validation (R^2_{val}) was used to explain the percentage of variation. Although this is not the only requirement for a model to be considered accurate, it is necessary for the respective R^2 value to be as close to 1 as possible. On the contrary, low values are indicative of either poor correlation between spectra and the

reference values or poor reproducibility in the reference methods themselves [15]. Another value used was the root mean square error (RMSE), which is a measure of the difference between predicted values and the true values determined by the reference methods [22]. This value, therefore, provides the average prediction error and is reported in the same units as the reference values. Values are reported for both calibration (RMSECV) and prediction (RMSEP) [23]. Residual predictive deviation (RPD) is the ratio of standard deviation of the data set to the RMSE and is calculated as the standard deviation of the population divided by the root mean standard error for both calibration (RPDcal) and validation (RPDval) [24]. The higher the RPD, the higher the ability of the model to accurately predict new samples.

Further, slope and intercept tests, as reported by Linnet [25], were used in each case to determine if systematic error existed between the predicted values and reference values or if the differences were a product of random noise. This method of analysis makes no assumptions regarding which set of values is the reference. The null hypothesis is accepted if the slope is found to be 1 and the y-intercept is found to be 0 at 95% confidence intervals. This test is used to compare the predicted values and the reference values for a particular model and the predicted values for sample treatments as well as different instruments. The inter-class correlation (ICC) is a value that is used to determine the consistency values predicted by the models and was used in the validations of the models and in the comparisons between sample treatments and instruments [26]. ICC can range from 0 to 1, where a value of 1 indicates perfect reliability, and, therefore, values as close to 1 as possible are desirable. Finally, the standard error of measurement (SEM) was also used to validate the models. This method can determine the precision of each individual measurement, and can, therefore, provide an absolute value of the reliability of a model [22].

The limit of detection (LOD) and limit of quantification (LOQ) of the PLS calibrations were also calculated and used to determine at which point in the fermentation the model could be accurately applied. The regression coefficients of the calculated PLS regression model are used in conjunction with the standard deviations (uncertainties) of the reference and spectroscopic methods to calculate the LOD and LOQ. This is possible as the LOD is an indication of the lowest concentration of an analyte that can be detected and therefore accurately predicted. The LOQ is calculated at three times the LOD [27].

3. Results

3.1. Reference Data

Previous research indicated that a coefficient of variance (CV) higher than 30% can be used as an indication of variability contained within the sample set [14,28]. Table 1 summarizes the statistics for the reference data, compiled from 324 samples, that were used for the study. From Table 1, except in the case of methylcellulose precipitate tannins, all the phenolic parameters have large coefficients of variation (CV). The high CV together with the gradual extraction of phenolic compounds during the fermentation process provides enough variability in the data set to attempt PLS regression modelling. The ranges for anthocyanins and polymeric pigments are consistent with those reported in the literature and therefore can be considered typical of South African red wines. However, the maximum value of the colour density, MCP tannins and TPI ranges are lower than those reported.

Table 1. Summary Statistics of Phenolic Parameters for Must and Wine.

Variable	Minimum	Maximum	Mean	Standard Deviation	CV
Anthocyanin (mg/L)	22.58	874.51	450.56	227.00	50.38
Colour Density (AU ₄₂₀₊₅₂₀₊₆₂₀)	0.33	33.63	17.13	9.97	58.22
MCP Tannins (mg/L)	507.10	1400.00	820.84	202.45	24.66
Polymeric Pigments (mg/L)	1.36	166.75	63.87	46.71	73.14
Total Polyphenol Index (AU ₂₈₀)	3.94	67.42	38.13	16.43	43.06

3.2. ATR-FT-MIR Prediction Models

The mid-infrared region provides fundamental vibrational frequencies for certain functional groups in molecules [29,30]. There are certain bands within this region that correspond with different components in wine. Water, ethanol, and carbon dioxide are associated with bands at 3305 cm^{-1} and 1640 cm^{-1} , 2985 cm^{-1} and 1050 cm^{-1} , and 2341 cm^{-1} , respectively [14]. The region associated with phenolic compounds, the fingerprint region, has been reported to be between $1500\text{--}900\text{ cm}^{-1}$ [23].

When considering the R^2 values for a predictive model, a value above 0.8 indicates a high degree of correlation [31]. For the ATR-FT-MIR technique, all ten models showed a high degree of correlation as seen in Table 2 along with other relevant statistics. RPD values ranging from 1.5–2.5 might be considered suitable for industrial purposes [15], although only for screening, while those above 2.5 might be considered of sufficient accuracy for the prediction of compounds [32]. The RPD statistic is somehow controversial as varying ranges of accuracy have been reported in the literature. The values presented here were used in the context of this application and they should therefore not be extrapolated to different applications. Again, eight of the ten models showed RPDvals that were all adequate for predictions. However, in the case of MCP tannins, these values were instead 2.21 for filtered samples and 2.33 for untreated samples, showing lower performance. However, for this application, these models could still be considered suitable. The null hypothesis for the models was in most cases accepted. This indicates that differences between the true and predicted values for the models can be considered negligible. To further analyse the reliability and accuracy of the models, the ICC and SEM were investigated. It was found that 80% of the models had an ICC of over 0.9 while the SEM was in the same magnitude and lower than the RMSEP. The models used to predict the MCP tannins had ICC values of 0.88 and 0.89 for untreated and filtered samples, respectively, but had SEM values lower than the RMSE, which might suggest model reliability [15]. When exploring the LOD and LOQ, it was found that all the models except for the one developed for anthocyanins in a filtered sample had LODs lower than the lowest predicted value. The low values of the LOD indicates that they can be used for prediction during the full course of a fermentation.

Different spectral pre-processing were selected based on which resulted in the best performance for each compound, and these can be seen in Supplementary Material Table S1a. The wavenumber regions selected using the iPLS interval selections included the fingerprint region for phenolic compounds. In five of the cases, other regions between $2500\text{--}4000\text{ cm}^{-1}$ were also selected, which is consistent with the absorption of IR radiation for phenolic compounds such as tannins [33].

Table 2. Summary statistics for filtered and untreated samples using attenuated-reflection Fourier-transform mid-infrared (ATR-FT-MIR) spectroscopy.

Component	Treatment	Rank	N	R ² _{Cal}	R ² _{Val}	RPD _{Cal}	RPD _{Val}	RMSEC	RMSEP	SEM	Bias	SI	ICC	LOD	LOQ
Anthocyanins (mg/L)	Filtered	7	214	0.926	0.8877	3.77	2.97	60.85	77.24	54.431	−9.82	Ho Accepted	0.94	7.22–15.13	21.65–45.39
Anthocyanins (mg/L)	Untreated	8	209	0.836	0.853	2.47	2.61	90.11	85.72	60.858	−3.73	Ho Accepted	0.924	5.06–13.98	15.17–41.93
Colour Density (AU ₄₂₀₊₅₂₀₊₆₂₀)	Filtered	6	214	0.924	0.901	3.65	3.21	2.69	3.19	2.27	0.13	Ho Accepted	0.949	0.35–1.05	1.04–3.16
Colour Density (AU ₄₂₀₊₅₂₀₊₆₂₀)	Untreated	4	209	0.914	0.889	3.43	3	2.87	3.33	2.369	−0.03	Ho Accepted	0.944	0.26–0.40	0.77–1.19
Polymeric Pigments (mg/L)	Filtered	8	214	0.894	0.882	3.09	2.92	15.37	15.53	11.019	−0.83	Ho Accepted	0.938	0.74–2.37	2.21–7.12
Polymeric Pigments (mg/L)	Untreated	7	209	0.906	0.874	3.06	2.82	14.53	15.92	11.288	1.18	Ho Accepted	0.934	0.74–2.80	2.23–8.41
Tannins (mg/L)	Filtered	5	214	0.79	0.804	2.19	2.21	91.33	92.11	65.431	−1.72	Ho Rejected	0.884	38.70–56.06	116.11–168.19
Tannins (mg/L)	Untreated	3	209	0.768	0.816	2.08	2.33	95.89	85.23	60.459	5.17	Ho Rejected	0.895	38.09–45.73	117.27–137.20
TPI (AU ₂₈₀)	Filtered	9	214	0.894	0.9	3.09	3.18	5.24	5.22	4.766	0.04	Ho Accepted	0.921	0.48–1.28	1.36–3.83
TPI (AU ₂₈₀)	Untreated	8	209	0.924	0.922	3.67	3.58	4.47	4.53	3.141	0.26	Ho Accepted	0.963	0.96–1.32	2.06–3.95

TPI: total polyphenol index; N: number of samples used in the development of the calibration model; R²_{cal}: coefficient of determination in calibration; R²_{val}: coefficient of determination in validation RPD_{cal}: residual predictive deviation in calibration; RPD_{val}: residual predictive deviation in validation; RMSEC and RMSEP: root mean square error of calibration and prediction, respectively; SEM; standard error of measurement; SI: Slope–Intercept with acceptance or rejection of the null-hypothesis (Ho); ICC: interclass correlation coefficients; LOD: limit of detection; LOQ: limit of quantification.

3.3. Transmission Fourier-Transform near-Infrared (T-FT-NIR) Prediction Models

Vibrational information given when using the NIR region of the electromagnetic spectrum is in the form of combination bands and overtones. Single compounds form characteristic bands within the spectrum, making this a highly suitable technique for analytical quantification [30]. Water and ethanol can be seen at wavenumbers of 6900 cm^{-1} and 5100 cm^{-1} , respectively. The region surrounding 5600 cm^{-1} is associated with the main sugars in juice as well as phenolic compounds present in red wine [34].

The R^2 values reported were in this case lower than those reported for the ATR-FT-MIR models. However, as seen in Table 3, only four of the models showed values below 0.8 and these were for both the anthocyanin models and TPI and MCP tannins for untreated samples. The RPDval values were lower than those for the ATR-FT-MIR models, and only two of those built had an RPDval higher than 2.5. Regarding the slope and intercept testing, the null hypothesis was rejected for all but three models. This indicates that there were significant differences between the true and predicted values for these compounds. This can be attributed to the light interference of the solids in suspension that are present in the samples. Even with the rejection of the null hypothesis in most of the cases, the ICC was still greater than 0.9 and the SEM was lower. The ICC values can indicate that the differences are due to the variance in the true vs. predicted values, whereas the SEM values indicate a certain level of accuracy.

LOD and LOQ values for these models were also investigated. In only six of the cases was the LOD lower than the lowest predicted value, indicating that the model may be inaccurate at lower concentrations of the analyte in question. This can also show that the models may suffer from inaccuracies in the first few days of fermentation and that they should rather be used from the middle to later stages of fermentation.

As with the previous spectroscopic technique, different pre-processing techniques were used when building the models. The method that was used most frequently was the baseline correction with automatic weighted least squares, with median centring being the second most frequently used technique. Wavenumber regions were identified by the iPLS interval selection, and these were $5800\text{--}6000\text{ cm}^{-1}$, $7000\text{--}8000\text{ cm}^{-1}$, $8500\text{--}9500\text{ cm}^{-1}$ and $10000\text{--}11500\text{ cm}^{-1}$. The rank, pre-processing methods and interval selections can be found in Supplementary information Table S1b. The regions identified by the iPLS do include the region near 5600 cm^{-1} , which is known to correlate to phenolic compounds.

Table 3. Summary statistics for filtered and untreated samples using transmission Fourier-transform near-infrared (T-FT-NIR) spectroscopy.

Component	Treatment	Rank	N	R ² _{Cal}	R ² _{Val}	RPD _{Cal}	RPD _{Val}	RMSEC	RMSEP	SEM	Bias	SI	ICC	LOD	LOQ
Anthocyanins (mg/L)	Filtered	4	236	0.709	0.729	1.85	1.89	121.03	128.86	89.16	−30.32	Ho Rejected	0.839	89.54–92.01	268.62–276.03
Anthocyanins (mg/L)	Untreated	4	208	0.576	0.652	1.54	1.62	145.4	143.25	97.87	−39.33	Ho Rejected	0.759	62.26–68.53	186.77–205.60
Colour Density (AU ₄₂₀₊₅₂₀₊₆₂₀)	Filtered	5	236	0.838	0.882	2.49	2.85	3.96	3.74	2.615	−0.72	Ho Rejected	0.931	2.76–7.50	8.29–22.49
Colour Density (AU ₄₂₀₊₅₂₀₊₆₂₀)	Untreated	5	208	0.835	0.822	2.48	2.38	3.97	4.26	3.03	−0.15	Ho Rejected	0.903	8.35–8.65	25.05–25.94
Polymeric Pigments (mg/L)	Filtered	3	236	0.8	0.827	2.24	2.4	21.29	18.63	13.19	1.98	Ho Accepted	0.908	3.04–3.28	9.12–9.84
Polymeric Pigments (mg/L)	Untreated	4	208	0.813	0.811	2.32	2.26	20.523	19.83	13.98	2.51	Ho Accepted	0.9	7.02–7.46	21.06–22.39
Tannins (mg/L)	Filtered	2	236	0.785	0.836	2.16	2.46	95.03	82.11	57.90	11.33	Ho Rejected	0.908	37.07–40.45	111.22–121.34
Tannins (mg/L)	Untreated	7	208	0.815	0.748	2.33	1.99	87.12	100.37	70.73	12.89	Ho Rejected	0.855	54.19–78.21	162.57–234.62
TPI (AU ₂₈₀)	Filtered	4	236	0.863	0.858	2.71	2.62	6.01	6.7	4.77	−0.36	Ho Accepted	0.921	21.94–22.39	65.81–67.18
TPI (AU ₂₈₀)	Untreated	3	208	0.71	0.757	1.86	2.11	8.58	8.47	6.01	−0.48	Ho Rejected	0.844	27.74–31.46	83.21–94.38

TPI: total polyphenol index; N: number of samples used in the development of the calibration model; R²_{cal}: coefficient of determination in calibration; R²_{val}: coefficient of determination in validation RPD_{cal}: residual predictive deviation in calibration; RPD_{val}: residual predictive deviation in validation; RMSEC and RMSEP: root mean square error of calibration and prediction, respectively; SEM; standard error of measurement; SI: Slope–Intercept with acceptance or rejection of the null-hypothesis (Ho); ICC: interclass correlation coefficients; LOD: limit of detection; LOQ: limit of quantification.

3.4. Diffuse-Reflectance Fourier-Transform near-Infrared (DR-FT-NIR) Prediction Models

As shown in Table 4, R^2 values higher than 0.8 were observed, indicating a high degree of correlation. In addition, seven of the ten models showed an RPD_{val} above 2.5. However, the models built for the prediction of tannins in both untreated and filtered samples and total phenolic index of untreated samples had lower RPD_{val} values (2.29, 2.33 and 2.3, respectively). Only 50% of the models had a positive result for the slope and intercept test, which indicates that errors between the models and the reference values are not negligible. However, this cannot quantify the magnitude of this error. To investigate the reliability of the models, the ICC was used in conjunction with the SEM. For this IR technique, 70% of the models showed an ICC above 0.9, with the remainder still being above 0.85. The ICC values show that the error observed is more likely due to the variance of the true versus the predicted values. Lastly, the SEM was in the same order of magnitude as the RMSE, and it was lower in every case, which could be indicative of increased accuracy.

The LOD in all cases was lower than the lowest predicted concentration. The LOQ in all cases was also lower than the lowest predicted concentration. It is important to note that the first sample of the reference data set used to build the model was collected immediately after crushing. This indicates that the models may be used from the first day of fermentation. The results indicate that the models are accurate and reliable throughout the entire fermentation, allowing for better control of the process.

The different pre-processing methods and wavenumber regions used can be seen in Supplementary Information Table S1c. Several different pre-processing methods were applied for the different models, the most common being the Multiway Scaling method. The wavenumber selections in all cases included the region 4100–12,000 cm^{-1} , which used most of the spectrum.

Table 4. Summary Statistics for filtered and turbid samples using direct-reflection Fourier-transform near-infrared (DR-FT-NIR) spectroscopy.

Component	Sample Treatment	Rank	N	R ² _{Cal}	R ² _{Val}	RPD _{Cal}	RPD _{Val}	RMSEC	RMSEP	SEM	Bias	SI	ICC	LOD	LOQ
Anthocyanins (mg/L)	Filtered	9	212	0.89	0.901	3.03	3.11	74.19	73.77	52.419	−0.34	Ho Accepted	0.95	5.01–18.25	15.03–54.74
Anthocyanins (mg/L)	Untreated	8	213	0.849	0.883	2.58	2.9	86.06	78.56	55.233	−0.22	Ho Rejected	0.937	5.05–11.23	15.16–33.68
Colour Density (AU ₄₂₀₊₅₂₀₊₆₂₀)	Filtered	7	212	0.901	0.889	3.18	3.01	3.07	3.39	2.406	0.19	Ho Accepted	0.942	0.83–1.16	2.50–3.48
Colour Density (AU ₄₂₀₊₅₂₀₊₆₂₀)	Untreated	7	213	0.864	0.887	2.72	3	3.59	3.4	2.419	0.17	Ho Accepted	0.942	0.26–0.58	0.79–1.74
Polymeric Pigments (mg/L)	Filtered	7	212	0.887	0.868	2.99	2.74	15.84	16.71	11.802	−1.84	Ho Accepted	0.931	0.75–3.61	2.24–10.83
Polymeric Pigments (mg/L)	Untreated	3	213	0.962	0.957	5.1	4.78	9.24	9.64	6.811	2	Ho Rejected	0.977	0.75–1.56	2.24–4.67
Tannins (mg/L)	Filtered	6	212	0.791	0.81	2.19	2.29	91.34	90.32	63.889	1.08	Ho Rejected	0.892	38.88–57.02	116.64–171.05
Tannins (mg/L)	Untreated	6	213	0.763	0.823	2.05	2.33	97.348	89.69	63.73	−1.26	Ho Rejected	0.889	38.82–51.53	116.45–154.60
TPI (AU ₂₈₀)	Filtered	8	212	0.879	0.91	2.88	3.33	5.64	5.04	3.567	−0.5	Ho Accepted	0.954	0.49–1.51	1.38–4.53
TPI (AU ₂₈₀)	Untreated	7	213	0.795	0.809	2.21	2.3	7.26	7.25	5.152	0.05	Ho Rejected	0.895	0.48–1.86	1.45–5.57

TPI: total polyphenol index; N: number of samples used in the development of the calibration model; R²_{cal}: coefficient of determination in calibration; R²_{val}: coefficient of determination in validation RPD_{cal}: residual predictive deviation in calibration; RPD_{val}: residual predictive deviation in validation; RMSEC and RMSEP: root mean square error of calibration and prediction, respectively; SEM; standard error of measurement; SI: Slope–Intercept with acceptance or rejection of the null-hypothesis (Ho); ICC: interclass correlation coefficients; LOD: limit of detection; LOQ: limit of quantification.

3.5. Instrument and Sample-Treatment Comparison

For instrument comparison, slope and intercept tests were performed and the ICC and SEM were explored, and the summary of these can be seen in Table 5. Of the pairwise comparisons for both sample treatments, the null hypothesis was confirmed for 66% of the cases. In the cases where the null hypothesis was accepted, this shows that the differences between the values predicted by different instruments is due to random noise rather than an existing systematic error. In all the cases where the null hypothesis was rejected, the T-FT-NIR technique was found to be in common. This could be because for this technique, the presence of turbidity in the form of solid particles of the sample negatively interferes with the infrared scanning.

A summary of the statistics comparing the sample treatments for each instrument can be found in Table 6. For the ATR-MIR instrument, the differences in predicted values for the sample treatments can be seen to be a product of random noise. This is confirmed by the accepted null hypothesis for each component as well as ICC values that are consistently higher than 0.9 and SEM values that are within the RMSEP values reported. This may be in part due to the way in which ATR-MIR spectroscopy functions, as well as the spectral pre-processing reducing the interference, which may have been caused by solids present in the sample.

For the T-FT-NIR, the null hypothesis was rejected for anthocyanins and total phenolic index. The accepted null hypothesis in the other models and the similar values for ICC and SEM (Table 3) suggest that the differences are simply a product of random noise for these parameters. This might indicate that the presence of solids in suspension does not have an effect when predicting certain components, whereas, for anthocyanins and total phenolic index, the interference plays a significant role. As the solid components present in the samples are primarily grape skin and yeast cells, these solids possibly containing reabsorbed anthocyanin molecules could be a plausible explanation for these results.

The statistics given for the DF-FT-NIR also suggest that the turbidity plays a significant role with the predicted values. As this spectroscopic technique is reliant on the presence of solids in order to function correctly, it was expected that a certain degree of solids in suspension would improve the model performance.

Table 5. Summary Statistics for Instrument Comparison for the phenolic parameters evaluated.

Treatment	Component	Comparison	SI	ICC	SEM
Filtered	Anthocyanins (mg/L)	ATR-FT-MIR/T-FT-NIR	Ho Accepted	0.811	90.09
		ATR-FT-MIR/DR-FT-NIR	Ho Accepted	0.833	92.25
		T-FT-NIR/DR-FT-NIR	Ho Accepted	0.834	90.16
	Colour Density (AU ₄₂₀₊₅₂₀₊₆₂₀)	ATR-FT-MIR/T-FT-NIR	Ho Rejected	0.861	3.303
		ATR-FT-MIR/DR-FT-NIR	Ho Accepted	0.935	2.468
		T-FT-NIR/DR-FT-NIR	Ho Accepted	0.897	3.003
	Polymeric Pigments (mg/L)	ATR-FT-MIR/T-FT-NIR	Ho Rejected	0.875	9.52
		ATR-FT-MIR/DR-FT-NIR	Ho Accepted	0.938	10.819
		T-FT-NIR/DR-FT-NIR	Ho Rejected	0.851	10.249
	Tannins (mg/L)	ATR-FT-MIR/T-FT-NIR	Ho Rejected	0.737	66.333
		ATR-FT-MIR/DR-FT-NIR	Ho Accepted	0.93	47.064
		T-FT-NIR/DR-FT-NIR	Ho Rejected	0.745	68.207
	TPI (AU ₂₈₀)	ATR-FT-MIR/T-FT-NIR	Ho Accepted	0.879	4.581
		ATR-FT-MIR/DR-FT-NIR	Ho Accepted	0.958	3.303
		T-FT-NIR/DR-FT-NIR	Ho Accepted	0.869	4.796
Untreated	Anthocyanins (mg/L)	ATR-FT-MIR/T-FT-NIR	Ho Rejected	0.821	81.508
		ATR-FT-MIR/DR-FT-NIR	Ho Accepted	0.887	72.118
		T-FT-NIR/DR-FT-NIR	Ho Rejected	0.767	92.018
	Colour Density (AU ₄₂₀₊₅₂₀₊₆₂₀)	ATR-FT-MIR/T-FT-NIR	Ho Rejected	0.939	2.36
		ATR-FT-MIR/DR-FT-NIR	Ho Accepted	0.953	2.129
		T-FT-NIR/DR-FT-NIR	Ho Accepted	0.912	2.818
	Polymeric Pigments (mg/L)	ATR-FT-MIR/T-FT-NIR	Ho Accepted	0.929	11.462
		ATR-FT-MIR/DR-FT-NIR	Ho Accepted	0.893	14.18
		T-FT-NIR/DR-FT-NIR	Ho Accepted	0.852	16.792
	Tannins (mg/L)	ATR-FT-MIR/T-FT-NIR	Ho Accepted	0.902	53.353
		ATR-FT-MIR/DR-FT-NIR	Ho Accepted	0.916	49.972
		T-FT-NIR/DR-FT-NIR	Ho Accepted	0.875	60.205
	TPI (AU ₂₈₀)	ATR-FT-MIR/T-FT-NIR	Ho Rejected	0.88	5.059
		ATR-FT-MIR/DR-FT-NIR	Ho Accepted	0.908	4.709
		T-FT-NIR/DR-FT-NIR	Ho Rejected	0.814	6.074

ATR-FT-MIR: attenuated-total-reflection Fourier-transform mid-infrared; T-FT-NIR: transmission Fourier-transform near-infrared; DR-FT-NIR: direct-reflection Fourier-transform near-infrared; SEM; standard error of measurement; SI: Slope–Intercept with acceptance or rejection of the null-hypothesis (Ho); ICC: interclass correlation coefficients.

Table 6. Summary Statistics for Sample-Treatment Comparison.

ATR-FT-MIR				
Component	Comparison	SI	ICC	SEM
Anthocyanins (mg/L)	Filtered/Untreated	Ho Accepted	0.939	55.661
Colour Density (AU ₄₂₀₊₅₂₀₊₆₂₀)	Filtered/ Untreated	Ho Accepted	0.984	1.225
Polymeric Pigments (mg/L)	Filtered/ Untreated	Ho Accepted	0.979	5.873
Tannins (mg/L)	Filtered/ Untreated	Ho Accepted	0.949	35.882
TPI (AU ₂₈₀)	Filtered/ Untreated	Ho Accepted	0.978	2.35
T-FT-NIR				
Component	Comparison	SI	ICC	SEM
Anthocyanins (mg/L)	Filtered/Untreated	Ho Rejected	0.929	59.321
Colour Density (AU ₄₂₀₊₅₂₀₊₆₂₀)	Filtered/ Untreated	Ho Accepted	0.967	1.763
Polymeric Pigments (mg/L)	Filtered/ Untreated	Ho Accepted	0.893	13.786
Tannins (mg/L)	Filtered/ Untreated	Ho Accepted	0.929	46.16
TPI (AU ₂₈₀)	Filtered/ Untreated	Ho Rejected	0.888	5.2
DR-FT-NIR				
Component	Comparison	SI	ICC	SEM
Anthocyanins (mg/L)	Filtered/Untreated	Ho Rejected	0.82	86.131
Colour Density (AU ₄₂₀₊₅₂₀₊₆₂₀)	Filtered/ Untreated	Ho Accepted	0.929	2.608
Polymeric Pigments (mg/L)	Filtered/ Untreated	Ho Rejected	0.975	7.059
Tannins (mg/L)	Filtered/ Untreated	Ho Accepted	0.91	55.64
TPI (AU ₂₈₀)	Filtered/ Untreated	Ho Rejected	0.917	4.492

ATR-FT-MIR: attenuated-total-reflection Fourier-transform mid-infrared; T-FT-NIR: transmission Fourier-transform near-infrared; DR-FT-NIR: direct-reflection Fourier-transform near-infrared; SEM; standard error of measurement; SI: Slope–Intercept with acceptance or rejection of the null-hypothesis (Ho); ICC: interclass correlation coefficients.

4. Discussion

NIR and MIR spectroscopy is already beneficial in that it is rapid, non-destructive and requires very little sample preparation [11,35,36]. The incorporation of samples that are more representative of those taken directly from a tank is another step in moving towards better process control in the wine industry. Developed PLS regression models often make use of spectral pre-processing techniques to improve the accuracy and reliability of the models [7,9,14,37]. In addition, wavenumber selection is common when developing calibrations once fingerprint regions have been identified. Further, the applicability of a model is also dependent on the limit of detection, as this will determine at what point in the fermentation it can be applied. This metric has been reported in studies conducted on wine fermentations [7,15].

To our knowledge, this is the first study of its kind, seeking to use IR technology and chemometric techniques to optimise PLS regression models for phenolic compounds in minimally treated or untreated wine/must samples. A study by Shrake et al., 2014 demonstrated that non-destructive, in-line monitoring of colour and total phenolic content of red wine is a possibility, with very positive results. In this study, samples were filtered in line using a 2 µm filter and analysed using light-emitting-diode sensors. However, in this study, yeast and pulp were removed with the use of peristaltic pumps before scanning took place [38]. The remaining particles, therefore, did not exceed 2 µm in size when scanning took place. In contrast, this study incorporates samples where the size of the solid particulates is not controlled by means of a filter (untreated) or in samples where the size of the particles would not exceed 400 µm in size. This study, therefore, allows for more simplistic in-line monitoring, as finer filters would not need to be incorporated into the system for sampling purposes. However, one aspect addressed in Shrake et al., 2014, which would be beneficial to this study is the development of an in-line flow cell, which would replace the physical instrument.

New PLS calibrations for three different spectroscopic methods, namely ATR-FT-MIR, DR-FT-NIR, and T-FT-NIR, were optimised. The models for ATR-FT-MIR were shown to be suitable for use in industry, as they showed sufficient accuracy while also having an LOD and LOQ suitable for lower levels of phenolic compounds. This was the case for ATR-FT-MIR for samples that were filtered and those that received no treatment. This is consistent with how this spectroscopic method functions. As the IR radiation is only allowed to penetrate the sample by 2 μm [39], entrained gasses and solid particles are expected not to have a substantial influence when the spectra are obtained. In the case of ATR-FT-MIR, it appears that filtration is more desirable than completely untreated samples. Models with good performance metrics can be expected from instrumentation such as this in a setting where samples will be taken directly from a fermentation vessel. Of the three spectroscopic acquisition methods, the ATR-FT-MIR had the best performance, allowing for accuracy as well as versatility in monitoring a fermentation.

DF-FT-NIR spectroscopy relies on variations in direction and intensity in the IR radiation after it has reflected from a sample's surface [40]. When considering the PLS calibrations built, the most suitable models were those built with filtered samples, as these models showed good performance in all the metrics. For samples with higher levels of turbidity, the scattering may be too intense, causing lower performance. The spectral pre-processing allows for better LOD and LOQ whilst still ensuring that RPD values remain high enough for practicality and reliability. As with the ATR-FT-MIR, these models show promise with regards to industrial application.

In the case of T-FT-NIR, the performance was substantially lower than that of the other two techniques. The spectral pre-processing and wavenumber selection appeared to have little effect on model improvement when untreated samples were used, and the models built using these techniques showed higher LODs and LOQs in conjunction with lower RPD values. However, it should still be noted that in certain cases, namely for polymeric pigments and TPI, the models were still appropriate for industrial application. In these cases, it might be pertinent to include better filtration techniques to improve the accuracy and reliability of the other PLS calibrations relying on this method.

With the ease of using the instrument and a further reduction in necessary sample treatment, these calibrations can be applied to in-line sampling systems. When deploying models in an industrial setting, it would be beneficial to incorporate a more complete sample set during the modelling stage that consists of a range of different cultivars and fermenting samples with a wide enough range of values for each phenolic component. These models used in conjunction with process-control software can lead to the incorporation of alarms and warnings, thereby providing an easier way for winemakers to control their fermentations. As most of the models showed good performance and suitability, it would be beneficial to consider other aspects such as cost and ease of installation when selecting a final system to be deployed.

Supplementary Materials: The following supporting information can be downloaded at: <https://www.mdpi.com/article/10.3390/fermentation8050231/s1>, Table S1: Additional model parameters. Pre-processing and spectral regions selected.

Author Contributions: Conceptualization, H.N., W.d.T. and J.L.A.-T.; methodology, H.N., W.d.T. and J.L.A.-T.; software, K.L.; validation, K.L. and J.L.A.-T.; formal analysis, K.L.; investigation, K.L. and J.L.A.-T.; resources, J.L.A.-T.; data curation, K.L. and J.L.A.-T.; writing—original draft preparation, K.L.; writing—review and editing, H.N., W.d.T. and J.L.A.-T.; visualization, K.L. and J.L.A.-T.; supervision, H.N., W.d.T. and J.L.A.-T.; project administration, K.L. and J.L.A.-T.; funding acquisition, J.L.A.-T. All authors have read and agreed to the published version of the manuscript.

Funding: This research was funded by Winetech SA grant number [JT-NP19].

Informed Consent Statement: Not applicable.

Acknowledgments: The authors gratefully acknowledge Winetech South Africa for funding and support under the grant number (JT-NP19).

Conflicts of Interest: The authors declare no conflict of interest.

References

1. McGovern, P.; Jalabadze, M.; Batiuk, S.; Callahan, M.P.; Smith, K.E.; Hall, G.R.; Kvavadze, E.; Maghradze, D.; Rusishvili, N.; Bouby, L.; et al. Early Neolithic Wine of Georgia in the South Caucasus. *Proc. Natl. Acad. Sci. USA* **2017**, *114*, E10309–E10318. [[CrossRef](#)] [[PubMed](#)]
2. Cusmano, L.; Morrison, A.; Rabbellotti, R. Catching up Trajectories in the Wine Sector: A Comparative Study of Chile, Italy, and South Africa. *World Dev.* **2010**, *38*, 1588–1602. [[CrossRef](#)]
3. Lochner, E. The Evaluation of Fourier Transform Infrared Spectroscopy (FT-IR) for the Determination of Total Phenolics and Total Anthocyanins Concentrations of Grapes. Ph.D. Thesis, Stellenbosch University, Stellenbosch, South Africa, 2006.
4. Santos, I.; Bosman, G.; Aleixandre-Tudo, J.L.; du Toit, W. Direct Quantification of Red Wine Phenolics Using Fluorescence Spectroscopy with Chemometrics. *Talanta* **2022**, *236*, 122857. [[CrossRef](#)]
5. Bureau, S.; Cozzolino, D.; Clark, C.J. Contributions of Fourier-Transform Mid Infrared (FT-MIR) Spectroscopy to the Study of Fruit and Vegetables: A Review. *Postharvest Biol. Technol.* **2019**, *148*, 1–14. [[CrossRef](#)]
6. Cozzolino, D. The Role of Visible and Infrared Spectroscopy Combined with Chemometrics to Measure Phenolic Compounds in Grape and Wine Samples. *Molecules* **2015**, *20*, 726–737. [[CrossRef](#)] [[PubMed](#)]
7. Debebe, A.; Redi-Abshiro, M.; Chandravanshi, B.S. Non-Destructive Determination of Ethanol Levels in Fermented Alcoholic Beverages Using Fourier Transform Mid-Infrared Spectroscopy. *Chem. Cent. J.* **2017**, *11*, 27. [[CrossRef](#)] [[PubMed](#)]
8. Gishen, M.; Dambergs, R.; Cozzolino, D. Grape and Wine Analysis—Enhancing the Power of Spectroscopy with Chemometrics. *Aust. J. Grape Wine Res.* **2008**, *11*, 296–305. [[CrossRef](#)]
9. Lourenço, N.D.; Lopes, J.A.; Almeida, C.F.; Sarraguça, M.C.; Pinheiro, H.M. Bioreactor Monitoring with Spectroscopy and Chemometrics: A Review. *Anal. Bioanal. Chem.* **2012**, *404*, 1211–1237. [[CrossRef](#)]
10. Oliveira-Folador, G.; Bicudo, M.d.O.; de Andrade, E.F.; Renard, C.M.G.C.; Bureau, S.; de Castilhos, F. Quality Traits Prediction of the Passion Fruit Pulp Using NIR and MIR Spectroscopy. *Lwt* **2018**, *95*, 172–178. [[CrossRef](#)]
11. Cavaglia, J.; Schorn-García, D.; Giussani, B.; Ferré, J.; Busto, O.; Aceña, L.; Mestres, M.; Boqué, R. ATR-MIR Spectroscopy and Multivariate Analysis in Alcoholic Fermentation Monitoring and Lactic Acid Bacteria Spoilage Detection. *Food Control* **2020**, *109*, 106947. [[CrossRef](#)]
12. Cozzolino, D.; Dambergs, R.G. Wine and Beer. In *Infrared Spectroscopy for Food Quality Analysis and Control*; Elsevier: Amsterdam, The Netherlands, 2009; pp. 127–168. ISBN 9780128118160.
13. Setford, P.C.; Jeffery, D.W.; Grbin, P.R.; Muhlack, R.A. Factors Affecting Extraction and Evolution of Phenolic Compounds during Red Wine Maceration and the Role of Process Modelling. *Trends Food Sci. Technol.* **2017**, *69*, 106–117. [[CrossRef](#)]
14. Aleixandre-Tudo, J.L.; Nieuwoudt, H.; Aleixandre, J.L.; du Toit, W. Chemometric Compositional Analysis of Phenolic Compounds in Fermenting Samples and Wines Using Different Infrared Spectroscopy Techniques. *Talanta* **2018**, *176*, 526–536. [[CrossRef](#)] [[PubMed](#)]
15. Aleixandre-Tudo, J.L.; Nieuwoudt, H.; Olivieri, A.; Aleixandre, J.L.; du Toit, W. Phenolic Profiling of Grapes, Fermenting Samples and Wines Using UV-Visible Spectroscopy with Chemometrics. *Food Control* **2018**, *85*, 11–22. [[CrossRef](#)]
16. Patz, C.D.; Blicke, A.; Ristow, R.; Dietrich, H. Application of FT-MIR Spectrometry in Wine Analysis. *Anal. Chim. Acta* **2004**, *513*, 81–89. [[CrossRef](#)]
17. Lambrecht, K.; Nieuwoudt, H.; Du Toit, W.; Aleixandre-Tudo, J.L. Moving towards In-Line Monitoring of Phenolic Extraction during Red Wine Fermentations Using Infra-Red Spectroscopy Technology. Influence of Sample Preparation and Instrumentation. *J. Food Compos. Anal.* **2022**, *110*, 104542. [[CrossRef](#)]
18. Iland, P. *Techniques for Chemical Analyses and Quality Monitoring during Winemaking*; Iland, P., Ed.; Patrick Iland Wine Promotions: Campbelltown, Australia, 2000; ISBN 064638435X.
19. Bindon, K.A.; Kassara, S.; Cynkar, W.U.; Robinson, E.M.C.; Scrimgeour, N.; Smith, P.A. Comparison of Extraction Protocols to Determine Differences in Wine-Extractable Tannin and Anthocyanin in *Vitis Vinifera* L. Cv. Shiraz and Cabernet Sauvignon Grapes. *J. Agric. Food Chem.* **2014**, *62*, 4558–4570. [[CrossRef](#)]
20. Mercurio, M.D.; Dambergs, R.G.; Herderich, M.J.; Smith, P.A. High Throughput Analysis of Red Wine and Grape Phenolics—Adaptation and Validation of Methyl Cellulose Precipitable Tannin Assay and Modified Somers Color Assay to a Rapid 96 Well Plate Format. *J. Agric. Food Chem.* **2007**, *55*, 4651–4657. [[CrossRef](#)]
21. Li, S.Y.; Zhu, B.Q.; Li, L.J.; Duan, C.Q. Extensive and Objective Wine Color Classification with Chromatic Database and Mathematical Models. *Int. J. Food Prop.* **2017**, *20*, S2647–S2659. [[CrossRef](#)]
22. Williams, P.; Dardenne, P.; Flinn, P. Tutorial: Items to Be Included in a Report on a near Infrared Spectroscopy Project. *J. Near Infrared Spectrosc.* **2017**, *25*, 85–90. [[CrossRef](#)]
23. Fragoso, S.; Aceña, L.; Guasch, J.; Mestres, M.; Busto, O. Quantification of Phenolic Compounds during Red Winemaking Using FT-MIR Spectroscopy and PLS-Regression. *J. Agric. Food Chem.* **2011**, *59*, 10795–10802. [[CrossRef](#)]
24. Fragoso, S.; Aceña, L.; Guasch, J.; Busto, O.; Mestres, M. Application of FT-MIR Spectroscopy for Fast Control of Red Grape Phenolic Ripening. *J. Agric. Food Chem.* **2011**, *59*, 2175–2183. [[CrossRef](#)] [[PubMed](#)]
25. Linnet, K. Evaluation of Regression Procedures for Methods Comparison Studies. *Clin. Chem.* **1993**, *39*, 424–432. [[CrossRef](#)] [[PubMed](#)]

26. Weir, J.P. Quantifying Test-Retest Reliability Using the Intraclass Correlation Coefficient and the SEM. *J. Strength Cond. Res.* **2005**, *19*, 231–240. [[CrossRef](#)]
27. Allegrini, F.; Olivieri, A.C. IUPAC-Consistent Approach to the Limit of Detection in Partial Least-Squares Calibration. *Anal. Chem.* **2014**, *86*, 7858–7866. [[CrossRef](#)]
28. Aleixandre-Tudo, J.; Nieuwoudt, H.; Aleixandre, J.; Du Toit, W. Robust Ultraviolet-Visible (UV-Vis) Partial Least-Squares (PLS) Models for Tannin Quantification in Red Wine. *J. Agric. Food Chem.* **2015**, *63*, 1088–1098. [[CrossRef](#)]
29. Larkin, P. General Outline and Strategies for IR and Raman Spectral Interpretation. *Infrared Raman Spectrosc.* **2011**, *117*, 133. [[CrossRef](#)]
30. Ricci, A.; Parpinello, G.P.; Laghi, L.; Lambri, M.; Versari, A. Application of Infrared Spectroscopy to Grape and Wine Analysis. In *Infrared Spectroscopy: Theory, Developments and Applications*; Nova Science Publisher: Hauppauge, NY, USA, 2014; ISBN 9781629485232.
31. Aleixandre-Tudo, J.; Nieuwoudt, H.; du Toit, W. Towards On-Line Monitoring of Phenolic Content in Red Wine Grapes: A Feasibility Study. *Food Chem.* **2019**, *270*, 322–331. [[CrossRef](#)]
32. Santos, P.M.; Colnago, L.A. Comparison Among MIR, NIR, and LF-NMR Techniques for Quality Control of Jam Using Chemometrics. *Food Anal. Methods* **2018**, *11*, 2029–2034. [[CrossRef](#)]
33. Basalekou, M.; Kallithraka, S.; Tarantilis, P.A.; Kotseridis, Y.; Pappas, C. Ellagitannins in Wines: Future Prospects in Methods of Analysis Using FT-IR Spectroscopy. *Lwt* **2019**, *101*, 48–53. [[CrossRef](#)]
34. Cozzolino, D.; Kwiatkowski, M.J.; Parker, M.; Cynkar, W.U.; Dambergs, R.G.; Gishen, M.; Herderich, M.J. Prediction of Phenolic Compounds in Red Wine Fermentations by Visible and near Infrared Spectroscopy. *Anal. Chim. Acta* **2004**, *513*, 73–80. [[CrossRef](#)]
35. Canal, C.; Ozen, B. Monitoring of Wine Process and Prediction of Its Parameters with Mid-Infrared Spectroscopy. *J. Food Process Eng.* **2017**, *40*, e12280. [[CrossRef](#)]
36. Parpinello, G.P.; Ricci, A.; Arapitsas, P.; Curioni, A.; Moio, L.; Segade, S.R.; Ugliano, M.; Versari, A. Multivariate Characterisation of Italian Monovarietal Red Wines Using MIR Spectroscopy. *Oeno One* **2019**, *53*, 741–751. [[CrossRef](#)]
37. Preys, S.; Roger, J.M.; Boulet, J.C. Robust Calibration Using Orthogonal Projection and Experimental Design. Application to the Correction of the Light Scattering Effect on Turbid NIR Spectra. *Chemom. Intell. Lab. Syst.* **2008**, *91*, 28–33. [[CrossRef](#)]
38. Shrake, N.L.; Amirtharajah, R.; Brenneman, C.; Boulton, R.; Knoesen, A. In-Line Measurement of Color and Total Phenolics during Red Wine Fermentations Using a Light-Emitting Diode Sensor. *Am. J. Enol. Vitic.* **2014**, *65*, 463–470. [[CrossRef](#)]
39. Mirabella, F.M. *Practical Spectroscopy Series; Internal Reflection Spectroscopy: Theory and Applications*; CRC Press: Boca Raton, FL, USA, 1993.
40. Hapke, B. Reflectance Methods and Applications. In *Encyclopedia of Spectroscopy and Spectrometry*; Academic Press: Cambridge, MA, USA, 2010; pp. 931–935. ISBN 9780128032244.